

MULTIGRID PRECONDITIONING FOR DISCONTINUOUS GALERKIN DISCRETIZATIONS OF AN ELLIPTIC OPTIMAL CONTROL PROBLEM WITH A CONVECTION-DOMINATED STATE EQUATION

SIJING LIU AND VALERIA SIMONCINI

ABSTRACT. We consider discontinuous Galerkin methods for an elliptic distributed optimal control problem constrained by a convection-dominated problem. We prove global optimal convergence rates using an inf-sup condition, with the diffusion parameter ε and regularization parameter β explicitly tracked. We then propose a multilevel preconditioner based on downwind ordering to solve the discretized system. The preconditioner only requires two approximate solves of single convection-dominated equations using multigrid methods. Moreover, for the strongly convection-dominated case, only two sweeps of block Gauss-Seidel iterations are needed. We also derive a simple bound indicating the role played by the multigrid preconditioner. Numerical results are shown to support our findings.

1. INTRODUCTION

We consider the following elliptic optimal control problem. Let Ω be a bounded convex polygonal domain in \mathbb{R}^2 , $y_d \in L_2(\Omega)$ and β be a positive constant. Find

$$(1.1) \quad (\bar{y}, \bar{u}) = \underset{(y,u)}{\operatorname{argmin}} \left[\frac{1}{2} \|y - y_d\|_{L_2(\Omega)}^2 + \frac{\beta}{2} \|u\|_{L_2(\Omega)}^2 \right],$$

where (y, u) belongs to $H_0^1(\Omega) \times L_2(\Omega)$ and such that

$$(1.2) \quad a(y, v) = \int_{\Omega} uv \, dx \quad \forall v \in H_0^1(\Omega).$$

Here the bilinear form $a(\cdot, \cdot)$ is defined as

$$(1.3) \quad a(y, v) = \varepsilon \int_{\Omega} \nabla y \cdot \nabla v \, dx + \int_{\Omega} (\zeta \cdot \nabla y) v \, dx + \int_{\Omega} \gamma y v \, dx,$$

Date: June 14, 2024.

2020 Mathematics Subject Classification. 49J20, 49M41, 65N30, 65N55.

Key words and phrases. elliptic distributed optimal control problems, convection-dominated problems, multilevel preconditioners, discontinuous Galerkin methods.

where $\varepsilon > 0$, the vector field $\zeta \in [W^{1,\infty}(\Omega)]^2$ and the function $\gamma \in L_\infty(\Omega)$ is nonnegative. We assume

$$(1.4) \quad \gamma - \frac{1}{2} \nabla \cdot \zeta \geq \gamma_0 > 0 \quad \text{a.e. in } \Omega,$$

so that the problem (1.2) is well-posed. We mainly focus on the convection-dominated regime, namely, the case where $\varepsilon \ll \|\zeta\|_{0,\infty} := \|\zeta\|_{[L^\infty(\Omega)]^2}$.

Remark 1.1. Throughout the paper we will follow the standard notation for differential operators, function spaces and norms that can be found for example in [10, 13, 15].

It is well-known, see, e.g. [30, 41], that the solution of (1.1)-(1.2) is characterized by

$$(1.5a) \quad a(q, \bar{p}) = (\bar{y} - y_d, q)_{L_2(\Omega)} \quad \forall q \in H_0^1(\Omega),$$

$$(1.5b) \quad \bar{p} + \beta \bar{u} = 0,$$

$$(1.5c) \quad a(\bar{y}, z) = (\bar{u}, z)_{L_2(\Omega)} \quad \forall z \in H_0^1(\Omega),$$

where \bar{p} is the adjoint state. After eliminating \bar{u} (cf. [24]), we arrive at the saddle point problem

$$(1.6a) \quad (\bar{p}, z)_{L_2(\Omega)} + \beta a(\bar{y}, z) = 0 \quad \forall z \in H_0^1(\Omega),$$

$$(1.6b) \quad a(q, \bar{p}) - (\bar{y}, q)_{L_2(\Omega)} = -(y_d, q)_{L_2(\Omega)} \quad \forall q \in H_0^1(\Omega).$$

Note that the system (1.6) is unbalanced with respect to β since it only appears in (1.6a). This can be remedied by the following change of variables:

$$(1.7) \quad \bar{p} = \beta^{\frac{1}{4}} \tilde{p} \quad \text{and} \quad \bar{y} = \beta^{-\frac{1}{4}} \tilde{y}.$$

The resulting saddle point problem is

$$(1.8a) \quad (\tilde{p}, z)_{L_2(\Omega)} + \beta^{\frac{1}{2}} a(\tilde{y}, z)_{L_2(\Omega)} = 0 \quad \forall z \in H_0^1(\Omega),$$

$$(1.8b) \quad \beta^{\frac{1}{2}} a(q, \tilde{p})_{L_2(\Omega)} - (\tilde{y}, q)_{L_2(\Omega)} = -\beta^{\frac{1}{4}} (y_d, q)_{L_2(\Omega)} \quad \forall q \in H_0^1(\Omega).$$

1.1. Difficulties of designing and analyzing numerical methods for (1.8).

There are several difficulties regarding designing and analyzing numerical methods for (1.8). First, standard Galerkin methods for convection-dominated problems are known to be unstable and produce oscillations near the outflow boundary. Therefore, stabilization techniques are necessary to obtain any meaningful solutions of such problems. Moreover, the saddle point problem (1.8) consists of a forward problem (1.8a) with convection field ζ and a dual problem (1.8b) with convection field $-\zeta$. This distinct feature in optimal control problems plays an important role in designing

stable and accurate numerical methods. In fact, it has been shown in [29, 23] that the opposite convection fields in optimal control problems are nontrivial to handle. The boundary layers in both directions will propagate into the interior domain even if a stabilization technique is used (cf. [23]). This phenomenon is essentially different from the behaviors of boundary layers in single convection-dominated equations, in which it is well-known that the boundary layer will not propagate into the interior of the domain if proper stabilization techniques are utilized. One significant finding in [29] is that the weak treatment of the boundary conditions prevents the oscillations near the boundary layers from propagating into interior domain where the solution is smooth. Note that this can be done by using Nitsche's methods [33] or discontinuous Galerkin methods [29, 44].

1.2. Difficulties of designing efficient solvers for (1.8). Designing fast iterative solvers for the resulting discretized system from (1.8) is nontrivial, especially in the convection-dominated regime. In this work, we focus on designing multigrid methods. For single convection-diffusion-reaction equations, it is well known that designing robust multigrid methods is difficult (see Section 5.2). Designing and analyzing multigrid methods for saddle point problems like (1.8) is even more challenging, and proper preconditioners must be devised. In [6, 7, 8, 9, 31], the authors designed a class of block-diagonal preconditioners and performed rigorous analyses of the multigrid methods that converge in the energy norm. Other approaches can be found in [37, 40, 39, 38] and the references therein. However, almost all the preconditioners deteriorate in the convection-dominated regime. We refer to [32, 35] for a known robust preconditioner in the convection-dominated regime which is based on the Schur complement.

Our contributions in this paper are two-fold. First, we propose and analyze an upwind discontinuous Galerkin (DG) method for solving (1.8) where the diffusion parameter ε and regularization parameter β are explicitly tracked. We show that the DG methods are optimal, for fixed β , in the sense of

$$(1.9) \quad \|p - p_h\|_{1,\varepsilon} + \|y - y_h\|_{1,\varepsilon} \leq \begin{cases} O(h) & \text{if (1.2) is diffusion-dominated,} \\ O(h^{\frac{3}{2}}) & \text{if (1.2) is convection-dominated,} \\ O(h^2) & \text{if (1.2) is reaction-dominated,} \end{cases}$$

where the norm $\|\cdot\|_{1,\varepsilon}$ is defined in (3.18) and h is the meshsize of the triangulation. Here (p, y) are solutions to (2.9) and (p_h, y_h) are solutions to (3.16). Our analysis is based on an inf-sup condition [8] and a crucial boundedness result in [15]. Note that the control is not explicitly discretized, instead, we eliminate the control using the

adjoint state [24], and hence we have a saddle point problem involving the state and the adjoint state. This technique is well-known, and it can be found, for instance, in [8, 20, 19]. We would like to point out that our DG methods are identical to those in [28, 29, 44], where similar estimates to (1.9) were derived in [28]. However, in our analysis, we do not decouple the state and the adjoint state by using intermediate problems, instead, we utilize the inf-sup condition and analyze the state and the adjoint state simultaneously, which is different from the one in [28].

Secondly, we design an efficient preconditioner to solve the discretized system. We combine the block-structured preconditioner by Pearson and Wathen [35] with downwind ordering multigrid methods [21] to construct a highly efficient preconditioner. There are two advantages to combining DG methods with the preconditioner in [35]. First, the mass matrix of DG methods is block-diagonal, allowing the inverse of the mass matrix to be computed exactly. Second, the downwind ordering technique makes the multigrid methods with block Gauss-Seidel iteration almost an exact solver as $\varepsilon \rightarrow 0$. In particular, as $\varepsilon \rightarrow 0$, a single sweep of block Gauss-Seidel is almost an exact solver, eliminating the need for multigrid cycles in those cases. Overall, with these techniques, the implementation of our preconditioner is extremely efficient in the convection-dominated regime, which only consists of two multigrid solves of single convection-diffusion-reaction equations. In terms of the quality of the preconditioner, we provide a bound of the distance between the approximate preconditioner and the ideal preconditioner, which justifies the efficiency of our preconditioner. Note that we mainly focus on the case where $\varepsilon \rightarrow 0$ in this work, i.e., the convection-dominated case, instead of the case where $\beta \rightarrow 0$, which is in contrast to [35, 8]. Nonetheless, numerical results in Section 6 indicate that our preconditioner is also robust when $\beta \rightarrow 0$.

The rest of the paper is organized as follows. In Section 2, we discuss the properties of the continuous problem (1.8) and establish its well-posedness. In Section 3, we introduce the DG methods and derive the inf-sup condition as well as an important boundedness result. In Section 4, we establish concrete error estimates for the DG methods in the convection-dominated regime. We then propose a block preconditioner in Section 5, where a crucial downwind ordering multigrid method with block Gauss-Seidel smoothers is introduced. A simple estimate is also derived in Section 5 to illustrate the quality of our preconditioner. Finally, we provide some numerical results in Section 6 and end with some concluding remarks in Section 7.

Throughout this paper, we use C (with or without subscripts) to denote a generic positive constant that is independent of any mesh parameter, β and ε , unless otherwise stated. Also to avoid the proliferation of constants, we use the notation $A \lesssim B$ (or $A \gtrsim B$) to represent $A \leq (\text{constant})B$. The notation $A \approx B$ is equivalent to $A \lesssim B$ and $B \lesssim A$.

2. CONTINUOUS PROBLEM

We rewrite (1.8) in a concise form

$$(2.1) \quad \mathcal{B}((\tilde{p}, \tilde{y}), (q, z)) = -\beta^{\frac{1}{4}}(y_d, q)_{L_2(\Omega)} \quad \forall (q, z) \in H_0^1(\Omega) \times H_0^1(\Omega),$$

where

$$(2.2) \quad \mathcal{B}((p, y), (q, z)) = \beta^{\frac{1}{2}}a(q, p) - (y, q)_{L_2(\Omega)} + (p, z)_{L_2(\Omega)} + \beta^{\frac{1}{2}}a(y, z).$$

Let $\|p\|_{H_{\varepsilon, \beta}^1(\Omega)}$ be defined by

$$(2.3) \quad \|p\|_{H_{\varepsilon, \beta}^1(\Omega)}^2 = \beta^{\frac{1}{2}} \left(\varepsilon \|p\|_{H^1(\Omega)}^2 + \|p\|_{L_2(\Omega)}^2 \right) + \|p\|_{L_2(\Omega)}^2.$$

We have the following lemmas regarding the bilinear form \mathcal{B} with respect to the norm $\|\cdot\|_{H_{\varepsilon, \beta}^1(\Omega)}$.

Lemma 2.1. *We have*

$$(2.4) \quad \mathcal{B}((p, y), (q, z)) \lesssim \frac{1}{\sqrt{\varepsilon}} (\|p\|_{H_{\varepsilon, \beta}^1(\Omega)}^2 + \|y\|_{H_{\varepsilon, \beta}^1(\Omega)}^2)^{\frac{1}{2}} (\|q\|_{H_{\varepsilon, \beta}^1(\Omega)}^2 + \|z\|_{H_{\varepsilon, \beta}^1(\Omega)}^2)^{\frac{1}{2}}$$

for any $(p, y), (q, z) \in H_0^1(\Omega) \times H_0^1(\Omega)$.

Proof. It follows from integration by parts and Cauchy-Schwarz inequality (cf. [26, Chapter 9]) that

$$(2.5) \quad \begin{aligned} \mathcal{B}((p, y), (q, z)) &\leq \beta^{\frac{1}{2}} \varepsilon |p|_{H^1(\Omega)} |q|_{H^1(\Omega)} + \beta^{\frac{1}{2}} \|\boldsymbol{\zeta}\|_{0, \infty} \|p\|_{L_2(\Omega)} |q|_{H^1(\Omega)} \\ &\quad + \beta^{\frac{1}{2}} (\|\boldsymbol{\zeta}\|_{1, \infty} + \|\gamma\|_{\infty}) \|q\|_{L_2(\Omega)} \|p\|_{L_2(\Omega)} \\ &\quad + \beta^{\frac{1}{2}} \varepsilon |y|_{H^1(\Omega)} |z|_{H^1(\Omega)} + \beta^{\frac{1}{2}} \|\boldsymbol{\zeta}\|_{0, \infty} \|y\|_{L_2(\Omega)} |z|_{H^1(\Omega)} \\ &\quad + \beta^{\frac{1}{2}} (\|\boldsymbol{\zeta}\|_{1, \infty} + \|\gamma\|_{\infty}) \|y\|_{L_2(\Omega)} \|z\|_{L_2(\Omega)} \\ &\quad + \|q\|_{L^2(\Omega)} \|y\|_{L^2(\Omega)} + \|p\|_{L^2(\Omega)} \|z\|_{L^2(\Omega)} \\ &\lesssim (\|p\|_{H_{\varepsilon, \beta}^1(\Omega)}^2 + \|y\|_{H_{\varepsilon, \beta}^1(\Omega)}^2)^{\frac{1}{2}} \\ &\quad \times (\beta^{\frac{1}{2}} \|q\|_{H^1(\Omega)}^2 + \|q\|_{L_2(\Omega)}^2 + \beta^{\frac{1}{2}} \|z\|_{H^1(\Omega)}^2 + \|z\|_{L_2(\Omega)}^2)^{\frac{1}{2}} \\ &\lesssim \frac{1}{\sqrt{\varepsilon}} (\|p\|_{H_{\varepsilon, \beta}^1(\Omega)}^2 + \|y\|_{H_{\varepsilon, \beta}^1(\Omega)}^2)^{\frac{1}{2}} (\|q\|_{H_{\varepsilon, \beta}^1(\Omega)}^2 + \|z\|_{H_{\varepsilon, \beta}^1(\Omega)}^2)^{\frac{1}{2}}. \end{aligned}$$

□

Lemma 2.2. *We have*

$$(2.6) \quad \sup_{(q, z) \in H_0^1(\Omega) \times H_0^1(\Omega)} \frac{\mathcal{B}((p, y), (q, z))}{(\|q\|_{H_{\varepsilon, \beta}^1(\Omega)}^2 + \|z\|_{H_{\varepsilon, \beta}^1(\Omega)}^2)^{\frac{1}{2}}} \geq 2^{-\frac{1}{2}} (\|p\|_{H_{\varepsilon, \beta}^1(\Omega)}^2 + \|y\|_{H_{\varepsilon, \beta}^1(\Omega)}^2)^{\frac{1}{2}}$$

for any $(p, y) \in H_0^1(\Omega) \times H_0^1(\Omega)$.

Proof. Given (p, y) , we take $q = p - y$, $z = p + y$. We have

$$(2.7) \quad \begin{aligned} \mathcal{B}((p, y), (q, z)) &= \beta^{\frac{1}{2}} a(p, p) + (p, p) + (y, y) + \beta^{\frac{1}{2}} a(y, y) \\ &\gtrsim \|p\|_{H_{\varepsilon, \beta}^1(\Omega)}^2 + \|y\|_{H_{\varepsilon, \beta}^1(\Omega)}^2 \end{aligned}$$

where we use the fact $\gamma - \frac{1}{2} \nabla \cdot \zeta \geq \gamma_0 \geq 0$ a.e. in Ω . Also, due to the parallelogram law, we have,

$$(2.8) \quad (\|q\|_{H_{\varepsilon, \beta}^1(\Omega)}^2 + \|z\|_{H_{\varepsilon, \beta}^1(\Omega)}^2)^{\frac{1}{2}} = 2^{\frac{1}{2}} (\|p\|_{H_{\varepsilon, \beta}^1(\Omega)}^2 + \|y\|_{H_{\varepsilon, \beta}^1(\Omega)}^2)^{\frac{1}{2}}.$$

Combining (2.7) and (2.8), we immediately obtain (2.6). \square

Remark 2.3. According to standard saddle point theory [4, 11], Lemma 2.1 and Lemma 2.2 guarantee the well-posedness of the problem (2.1).

For the sake of generality, we shall also consider the following more general problem. Let $(p, y) \in H_0^1(\Omega) \times H_0^1(\Omega)$ satisfies

$$(2.9) \quad \mathcal{B}((p, y), (q, z)) = (f, q)_{L_2(\Omega)} + (g, z)_{L_2(\Omega)} \quad \forall (q, z) \in H_0^1(\Omega) \times H_0^1(\Omega),$$

where $(f, g) \in L_2(\Omega) \times L_2(\Omega)$ and \mathcal{B} is defined in (2.2).

3. DISCRETE PROBLEM

In this section we discretize the saddle point problem (1.8) by a DG method [2, 1, 12]. Let \mathcal{T}_h be a quasi-uniform and shape regular simplicial triangulation of Ω . The diameter of $T \in \mathcal{T}_h$ is denoted by h_T and $h = \max_{T \in \mathcal{T}_h} h_T$ is the mesh diameter. Let $\mathcal{E}_h = \mathcal{E}_h^b \cup \mathcal{E}_h^i$ where \mathcal{E}_h^i (resp., \mathcal{E}_h^b) represents the set of interior edges (resp., boundary edges).

We further decompose the boundary edges \mathcal{E}_h^b into the inflow part $\mathcal{E}_h^{b,-}$ and the outflow part $\mathcal{E}_h^{b,+}$ which are defined as follows,

$$(3.1) \quad \mathcal{E}_h^{b,-} = \{e \in \mathcal{E}_h^b : e \subset \{x \in \partial\Omega : \zeta(x) \cdot \mathbf{n}(x) < 0\}\},$$

$$(3.2) \quad \mathcal{E}_h^{b,+} = \mathcal{E}_h^b \setminus \mathcal{E}_h^{b,-}.$$

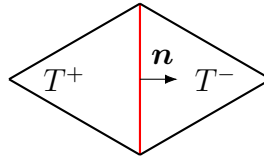


FIGURE 1. Interior edges

For an edge $e \in \mathcal{E}_h^i$, let h_e be the length of e . For each edge we associate a fixed unit normal \mathbf{n} . We denote by T^+ the element for which \mathbf{n} is the outward normal, and T^- the element for which $-\mathbf{n}$ is the outward normal (see Figure 1). We define the discontinuous finite element space V_h as

$$(3.3) \quad V_h = \{v \in L_2(\Omega) : v|_T \in \mathbb{P}_1(T) \quad \forall T \in \mathcal{T}_h\}.$$

For $v \in V_h$ on an edge e , we define

$$(3.4) \quad v^+ = v|_{T^+} \quad \text{and} \quad v^- = v|_{T^-}.$$

We define the jump and average for $v \in V_h$ on an edge e as follows,

$$(3.5) \quad [v] = v^+ - v^-, \quad \{v\} = \frac{v^+ + v^-}{2}.$$

For $e \in \mathcal{E}_h^b$ with $e \in \partial T$, we let

$$(3.6) \quad [v] = \{v\} = v|_T.$$

We also denote

$$(3.7) \quad (w, v)_e := \int_e wv \, ds \quad \text{and} \quad (w, v)_T := \int_T wv \, dx.$$

We introduce the following notation (cf. [15]):

$$(3.8) \quad \tau_c = \frac{1}{\max(\|\gamma\|_\infty, |\boldsymbol{\zeta}|_{1,\infty})}.$$

The quantity τ_c is useful in the convergence analysis. Note that τ_c is finite because $\|\gamma\|_\infty = |\boldsymbol{\zeta}|_{1,\infty} = 0$ implies $\gamma - \frac{1}{2}\nabla \cdot \boldsymbol{\zeta} = 0$, which contradicts our assumption (1.4).

3.1. Discontinuous Galerkin methods. DG methods for (2.1) aim to find $(\tilde{p}_h, \tilde{y}_h) \in V_h \times V_h$ such that

$$(3.9) \quad \mathcal{B}_h((\tilde{p}_h, \tilde{y}_h), (q, z)) = -(y_d, q)_{L_2(\Omega)} \quad \forall (q, z) \in V_h \times V_h,$$

where

$$(3.10) \quad \mathcal{B}_h((p, y), (q, z)) = \beta^{\frac{1}{2}} a_h(q, p) - (y, q)_{L_2(\Omega)} + (p, z)_{L_2(\Omega)} + \beta^{\frac{1}{2}} a_h(y, z).$$

The bilinear form $a_h(\cdot, \cdot)$ is defined by

$$(3.11) \quad a_h(u, v) = \varepsilon a_h^{\text{sip}}(u, v) + a_h^{\text{ar}}(u, v) \quad \forall u, v \in V_h,$$

where the term

$$(3.12) \quad \begin{aligned} a_h^{\text{sip}}(u, v) = & \sum_{T \in \mathcal{T}_h} (\nabla u, \nabla v)_T - \sum_{e \in \mathcal{E}_h} (\{\mathbf{n} \cdot \nabla u\}, [v])_e - \sum_{e \in \mathcal{E}_h} (\{\mathbf{n} \cdot \nabla v\}, [u])_e \\ & + \sigma \sum_{e \in \mathcal{E}_h} h_e^{-1} ([u], [v])_e \end{aligned}$$

is the bilinear form of the symmetric interior penalty (SIP) method with sufficiently large penalty parameter σ . The upwind DG scheme (cf. [12, 15]) for the advection-reaction term is defined as

$$(3.13) \quad a_h^{\text{ar}}(w, v) = \sum_{T \in \mathcal{T}_h} (\boldsymbol{\zeta} \cdot \nabla w + \gamma w, v)_T - \sum_{e \in \mathcal{E}_h^i} (\mathbf{n} \cdot \boldsymbol{\zeta} [w], v^{\text{down}})_e - \sum_{e \in \mathcal{E}_h^{b,-}} (\mathbf{n} \cdot \boldsymbol{\zeta} w, v)_e.$$

Here, the downwind value v^{down} of a function on an interior edge $e \in \mathcal{E}_h^i$ is defined as

$$(3.14) \quad v^{\text{down}} = \begin{cases} v^- & \text{if } \boldsymbol{\zeta} \cdot \mathbf{n} \geq 0, \\ v^+ & \text{if } \boldsymbol{\zeta} \cdot \mathbf{n} < 0. \end{cases}$$

Note that the scheme (3.13) is equivalent to the following,

$$(3.15) \quad \begin{aligned} a_h^{\text{ar}}(w, v) &= \sum_{T \in \mathcal{T}_h} (\boldsymbol{\zeta} \cdot \nabla w + \gamma w, v)_T - \sum_{e \in \mathcal{E}_h^i \cup \mathcal{E}_h^{b,-}} (\mathbf{n} \cdot \boldsymbol{\zeta} [w], \{v\})_e \\ &+ \sum_{e \in \mathcal{E}_h^i} \frac{1}{2} (|\boldsymbol{\zeta} \cdot \mathbf{n}| [w], [v])_e. \end{aligned}$$

DG methods for the more general problem (2.9) aim to find $(p_h, y_h) \in V_h \times V_h$ such that

$$(3.16) \quad \mathcal{B}_h((p_h, y_h), (q, z)) = (f, q)_{L_2(\Omega)} + (g, z)_{L_2(\Omega)} \quad \forall (q, z) \in V_h \times V_h.$$

In this context, we define the norm $\| \cdot \|$ as

$$(3.17) \quad \| \| v \| \|^2 = \beta^{\frac{1}{2}} \| v \|_{1,\varepsilon}^2 + \| v \|_{L_2(\Omega)}^2,$$

and the norm $\| \cdot \|_{1,\varepsilon}$ (cf. [15]) as

$$(3.18) \quad \| v \|_{1,\varepsilon}^2 := \| v \|_{H_\varepsilon^1(\Omega; \mathcal{T}_h)}^2 = \varepsilon \| v \|_d^2 + \| v \|_{ar}^2,$$

where

$$(3.19) \quad \| v \|_d^2 = \sum_{T \in \mathcal{T}_h} \| \nabla v \|_{L_2(T)}^2 + \sum_{e \in \mathcal{E}_h} \frac{1}{h_e} \| [v] \|_{L_2(e)}^2 + \sum_{e \in \mathcal{E}_h} h_e \| \{ \mathbf{n} \cdot \nabla v \} \|_{L_2(e)}^2$$

and

$$(3.20) \quad \| v \|_{ar}^2 = \tau_c^{-1} \| v \|_{L_2(\Omega)}^2 + \int_{\partial\Omega} \frac{1}{2} |\boldsymbol{\zeta} \cdot \mathbf{n}| v^2 ds + \sum_{e \in \mathcal{E}_h^i} \int_e \frac{1}{2} |\boldsymbol{\zeta} \cdot \mathbf{n}| [v]^2 ds.$$

3.2. The properties of $a_h(\cdot, \cdot)$. Let $V = H_0^1(\Omega) \cap H^2(\Omega)$. It is well-known that

$$(3.21) \quad a_h^{sip}(w, v) \lesssim \|w\|_d \|v\|_d \quad \forall w, v \in V + V_h,$$

$$(3.22) \quad a_h^{sip}(v, v) \gtrsim \|v\|_d^2 \quad \forall v \in V_h,$$

for sufficiently large σ (cf. [15, 10]). We also have ([15])

$$(3.23) \quad a_h^{ar}(v, v) \gtrsim \min(1, \gamma_0 \tau_c) \|v\|_{ar}^2 \quad \forall v \in V_h.$$

One can obtain (cf. [15, Lemma 2.30])

$$(3.24) \quad a_h^{ar}(w - \pi_h w, v) \lesssim \|w - \pi_h w\|_{ar,*} \|v\|_{ar} \quad \forall w \in V, v \in V_h,$$

for a stronger norm $\|\cdot\|_{ar,*}$ defined as

$$(3.25) \quad \|v\|_{ar,*}^2 = \|v\|_{ar}^2 + \sum_{T \in \mathcal{T}_h} \|\zeta\|_{0,\infty} \|v\|_{L_2(\partial T)}^2.$$

Here the operator $\pi_h : V \rightarrow V_h$ is the L_2 orthogonal projection. Note that the following is also true,

$$(3.26) \quad a_h^{ar}(v, w - \pi_h w) \lesssim \|w - \pi_h w\|_{ar,*} \|v\|_{ar} \quad \forall w \in V, v \in V_h.$$

Remark 3.1. The estimate (3.26) is not derived from (3.24) since $a_h^{ar}(\cdot, \cdot)$ is nonsymmetric. However, the technique used in [15, Lemma 2.30] to derive (3.24) can be employed to establish (3.26).

Overall, we have

$$(3.27) \quad a_h(w - \pi_h w, v) \lesssim \|w - \pi_h w\|_{1,\varepsilon,*} \|v\|_{1,\varepsilon} \quad \forall w \in V, v \in V_h,$$

$$(3.28) \quad a_h(v, w - \pi_h w) \lesssim \|w - \pi_h w\|_{1,\varepsilon,*} \|v\|_{1,\varepsilon} \quad \forall w \in V, v \in V_h,$$

$$(3.29) \quad a_h(v, v) \gtrsim \min(1, \gamma_0 \tau_c) \|v\|_{1,\varepsilon}^2 \quad \forall v \in V_h,$$

where the norm $\|\cdot\|_{1,\varepsilon,*}$ is defined as

$$(3.30) \quad \|\cdot\|_{1,\varepsilon,*}^2 = \varepsilon \|\cdot\|_d^2 + \|\cdot\|_{ar,*}^2.$$

3.3. The properties of \mathcal{B}_h . By (3.10), (3.29) and a direct calculation, we have

$$(3.31) \quad \begin{aligned} & \mathcal{B}_h((p, y), (p - y, p + y)) \\ &= \beta^{\frac{1}{2}} a_h(p, p) + (p, p)_{L_2(\Omega)} + (y, y)_{L_2(\Omega)} + \beta^{\frac{1}{2}} a_h(y, y) \\ & \gtrsim \min(1, \gamma_0 \tau_c) (\|p\|^2 + \|y\|^2) \end{aligned}$$

and

$$(3.32) \quad \|p - y\|^2 + \|p + y\|^2 = 2(\|p\|^2 + \|y\|^2)$$

by the parallelogram law. It follows from (3.31) and (3.32) that

$$(3.33) \quad \begin{aligned} & \|\|p_h\|\| + \|\|y_h\|\| \\ & \lesssim \frac{1}{\min(1, \gamma_0 \tau_c)} \sup_{(q,z) \in V_h \times V_h} \frac{\mathcal{B}_h((p_h, y_h), (q, z))}{\|\|q\|\| + \|\|z\|\|} \quad \forall (p_h, y_h) \in V_h \times V_h. \end{aligned}$$

Define the norm

$$(3.34) \quad \|\|v\|\|_*^2 = \beta^{\frac{1}{2}} \|v\|_{1,\varepsilon,*}^2 + \|v\|_{L_2(\Omega)}^2.$$

It follows from (3.17), (3.27), (3.28), and (3.25) that, for any $(p, y) \in V \times V$ and $(q, z) \in V_h \times V_h$,

$$(3.35) \quad \begin{aligned} & \mathcal{B}_h((p - \pi_h p, y - \pi_h y), (q, z)) \\ & = \beta^{\frac{1}{2}} a_h(q, p - \pi_h p) - (y - \pi_h y, q)_{L_2(\Omega)} + (p - \pi_h p, z)_{L_2(\Omega)} \\ & \quad + \beta^{\frac{1}{2}} a_h(y - \pi_h y, z) \\ & \lesssim \beta^{\frac{1}{2}} \|p - \pi_h p\|_{1,\varepsilon,*} \|q\|_{1,\varepsilon} + \|y - \pi_h y\|_{L_2(\Omega)} \|q\|_{L_2(\Omega)} \\ & \quad + \|p - \pi_h p\|_{L_2(\Omega)} \|z\|_{L_2(\Omega)} + \beta^{\frac{1}{2}} \|y - \pi_h y\|_{1,\varepsilon,*} \|z\|_{1,\varepsilon} \\ & \lesssim (\|\|p - \pi_h p\|\|_* + \|\|y - \pi_h y\|\|_*) (\|\|q\|\| + \|\|z\|\|). \end{aligned}$$

3.4. Consistency. It is well-known that the DG method (3.16) is consistent (cf. [2, 36, 10, 15]). In other words, we have the following Galerkin orthogonality,

$$(3.36) \quad \mathcal{B}_h((p - p_h, y - y_h), (q, z)) = 0 \quad \forall (q, z) \in V_h \times V_h,$$

where (p, y) is the solution to (2.9) and (p_h, y_h) is the solution to (3.16).

4. CONVERGENCE ANALYSIS OF DG METHODS

In this section, we establish concrete error estimates for the DG method (3.16). We first recall some preliminary results. For $T \in \mathcal{T}_h$ and $v \in H^{1+s}(T)$ where $s \in (\frac{1}{2}, 1]$, the following trace inequalities with scaling are standard (cf. [17, Lemma 7.2] and [14, Proposition 3.1]),

$$(4.1) \quad \|v\|_{L_2(\partial T)} \lesssim (h_T^{-\frac{1}{2}} \|v\|_{L_2(T)} + h_T^{s-\frac{1}{2}} |v|_{H^s(T)}),$$

$$(4.2) \quad \|\nabla v\|_{L_2(\partial T)} \lesssim (h_T^{-\frac{1}{2}} \|\nabla v\|_{L_2(T)} + h_T^{s-\frac{1}{2}} |\nabla v|_{H^s(T)}).$$

We then have the following standard projection estimate [10]. By (4.1), (4.2) and a standard inverse inequality, we obtain

$$(4.3) \quad \|z - \pi_h z\|_{L_2(\Omega)} + h \|z - \pi_h z\|_d \lesssim h^2 \|z\|_{H^2(\Omega)} \quad \forall z \in V.$$

It follows from (3.20) that

$$(4.4) \quad \|z - \pi_h z\|_{ar} \lesssim (\tau_c^{-\frac{1}{2}} h^2 + \|\zeta\|_{0,\infty}^{\frac{1}{2}} h^{\frac{3}{2}}) \|z\|_{H^2(\Omega)} \quad \forall z \in V.$$

We are ready to state our new error bound.

Theorem 4.1. *Let (p, y) be the solution to (2.9) and (p_h, y_h) be the solution to (3.16). We have,*

$$(4.5) \quad \begin{aligned} & \| \|p - p_h\| \| + \| \|y - y_h\| \| \\ & \lesssim C_{\dagger} \left(\beta^{\frac{1}{4}} (\varepsilon^{\frac{1}{2}} + \|\zeta\|_{0,\infty}^{\frac{1}{2}} h^{\frac{1}{2}} + \tau_c^{-\frac{1}{2}} h) h + h^2 \right) (\|p\|_{H^2(\Omega)} + \|y\|_{H^2(\Omega)}), \end{aligned}$$

where $C_{\dagger} = (1 + \frac{1}{\min(1, \gamma_0 \tau_c)})$.

Proof. It follows from (3.33), (3.35) and (3.36) that, for all $(p_h, y_h) \in V_h \times V_h$,

$$(4.6) \quad \begin{aligned} & \| \|p_h - \pi_h p\| \| + \| \|y_h - \pi_h y\| \| \\ & \lesssim \frac{1}{\min(1, \gamma_0 \tau_c)} \sup_{(q,z) \in V_h \times V_h} \frac{\mathcal{B}_h((p_h - \pi_h p, y_h - \pi_h y), (q, z))}{\| \|q\| \| + \| \|z\| \|} \\ & = \frac{1}{\min(1, \gamma_0 \tau_c)} \sup_{(q,z) \in V_h \times V_h} \frac{\mathcal{B}_h((p - \pi_h p, y - \pi_h y), (q, z))}{\| \|q\| \| + \| \|z\| \|} \\ & \lesssim \frac{1}{\min(1, \gamma_0 \tau_c)} (\| \|p - \pi_h p\| \|_* + \| \|y - \pi_h y\| \|_*). \end{aligned}$$

We then estimate the term $\| \|p - \pi_h p\| \|_*$; an estimate of the other term involving y will follow similarly. Combining (4.1), (4.3), (4.4) and (3.30), we obtain,

$$(4.7) \quad \begin{aligned} \| \|p - \pi_h p\| \|_*^2 &= \beta^{\frac{1}{2}} \left(\varepsilon \|p - \pi_h p\|_d^2 + \|p - \pi_h p\|_{ar}^2 + \sum_{T \in \mathcal{T}_h} \|\zeta\|_{0,\infty} \|p - \pi_h p\|_{L_2(\partial T)}^2 \right) \\ &+ \|p - \pi_h p\|_{L_2(\Omega)}^2 \\ &\lesssim \left(\beta^{\frac{1}{2}} (\varepsilon + \|\zeta\|_{0,\infty} h + \tau_c^{-1} h^2) h^2 + h^4 \right) \|p\|_{H^2(\Omega)}^2. \end{aligned}$$

It follows from (4.6), (4.7) and the triangle inequality that

$$(4.8) \quad \begin{aligned} & \| \|p - p_h\| \| + \| \|y - y_h\| \| \\ & \lesssim C_{\dagger} \left(\beta^{\frac{1}{4}} (\varepsilon^{\frac{1}{2}} + \|\zeta\|_{0,\infty}^{\frac{1}{2}} h^{\frac{1}{2}} + \tau_c^{-\frac{1}{2}} h) h + h^2 \right) (\|p\|_{H^2(\Omega)} + \|y\|_{H^2(\Omega)}). \end{aligned}$$

□

Remark 4.2. Theorem 4.1 indicates that our DG methods are optimal in the following sense,

$$(4.9) \quad \|p-p_h\|_{1,\varepsilon} + \|y-y_h\|_{1,\varepsilon} \leq \begin{cases} O(\beta^{\frac{1}{4}}h + h^2) & \text{if (1.2) is diffusion-dominated,} \\ O(\beta^{\frac{1}{4}}h^{\frac{3}{2}} + h^2) & \text{if (1.2) is convection-dominated,} \\ O(\beta^{\frac{1}{4}}h^2 + h^2) & \text{if (1.2) is reaction-dominated.} \end{cases}$$

Note that $\|p\|_{H^2(\Omega)} = O(\varepsilon^{-\frac{3}{2}})$ and $\|y\|_{H^2(\Omega)} = O(\varepsilon^{-\frac{3}{2}})$ ([29]), hence, the estimate (4.7) is not informative when $\varepsilon \leq h$. More delicate interior error estimates that stay away from the boundary layers and interior layers for standard DG methods can be found in [29].

Remark 4.3. The constant C_{\dagger} in Theorem 4.1 can be bounded independently of γ and ζ due to assumption (1.4). The purpose of keeping the constant is to track how the data of the state equation enters the estimate (4.5).

5. A ROBUST MULTIGRID PRECONDITIONER

In this section, we discuss block structured multigrid preconditioners to solve the discrete problem (3.16). Our experimental results illustrate their robustness. Let the triangulation $\mathcal{T}_1, \mathcal{T}_2, \dots$ be generated from the triangulation \mathcal{T}_0 through uniform subdivisions such that $h_k \approx \frac{1}{2}h_{k-1}$ and V_k be the DG space associated with \mathcal{T}_k . Let \mathbf{M}_k (resp., \mathbf{A}_k) denote the mass matrix representing the bilinear form $(\cdot, \cdot)_{L_2(\Omega)}$ (resp., $a_h(\cdot, \cdot)$) with respect to the natural discontinuous nodal basis in V_k . The discrete problem can be written in the following form,

$$(5.1) \quad \begin{pmatrix} \mathbf{M}_k & \beta^{\frac{1}{2}}\mathbf{A}_k \\ \beta^{\frac{1}{2}}\mathbf{A}_k^t & -\mathbf{M}_k \end{pmatrix} \begin{pmatrix} \mathbf{p} \\ \mathbf{y} \end{pmatrix} = \begin{pmatrix} \mathbf{f} \\ \mathbf{g} \end{pmatrix}.$$

Let $\mathbf{B}_k = \begin{pmatrix} \mathbf{M}_k & \beta^{\frac{1}{2}}\mathbf{A}_k \\ \beta^{\frac{1}{2}}\mathbf{A}_k^t & -\mathbf{M}_k \end{pmatrix}$. It has been shown in [35] that the following preconditioner based on the Schur complement is efficient for the problem (5.1),

$$(5.2) \quad \mathcal{P}_k = \begin{pmatrix} \mathbf{M}_k & \\ & \mathbf{M}_k + \beta\mathbf{A}_k^t\mathbf{M}_k^{-1}\mathbf{A}_k \end{pmatrix}.$$

In particular, it has been noticed that the eigenvalues of $\mathcal{P}_k^{-1}\mathbf{B}_k$ are $\{\frac{1-\sqrt{5}}{2}, 1, \frac{1+\sqrt{5}}{2}\}$. A good approximation of \mathcal{P}_k is the following preconditioner (cf. [35, Theorem 1]),

$$(5.3) \quad \tilde{\mathcal{P}}_k = \begin{pmatrix} \mathbf{M}_k & \\ & (\beta^{\frac{1}{2}}\mathbf{A}_k + \mathbf{M}_k)^t\mathbf{M}_k^{-1}(\beta^{\frac{1}{2}}\mathbf{A}_k + \mathbf{M}_k) \end{pmatrix}.$$

First in [35] and later by other authors in [32], these preconditioners were used to solve the problem (1.1)-(1.2). However, they both needed to approximate the mass matrix \mathbf{M}_k using specific techniques. In our case, the inverse of \mathbf{M}_k is trivial since the mass matrix for DG methods is block diagonal. For the Schur complement, one has to either efficiently approximate $(\mathbf{M}_k + \beta \mathbf{A}_h^t \mathbf{M}_k^{-1} \mathbf{A}_k)^{-1}$ or $(\beta^{\frac{1}{2}} \mathbf{A}_k + \mathbf{M}_k)^{-1}$. The former was accomplished by using isogeometric analysis [32] and the latter can be realized by multigrid [35]. Here we adopt the multigrid strategy proposed in [21] to efficiently approximate the Schur complement. Note that approximating $(\beta^{\frac{1}{2}} \mathbf{A}_k + \mathbf{M}_k)^{-1}$ is equivalent to approximately solving a single diffusion-convection-reaction equation.

The quality of the approximate preconditioner can be measured in terms of the distance from the ideal preconditioner, corresponding to the Schur complement $\mathbf{S}_k = \mathbf{M}_k + \beta \mathbf{A}_k^t \mathbf{M}_k^{-1} \mathbf{A}_k$. This distance is given by the spectral equivalence between the two matrices; see, e.g., [18]. In [35, Theorem 4.1] it was shown that if

$$\widehat{\mathbf{S}}_k := (\beta^{\frac{1}{2}} \mathbf{A}_k + \mathbf{M}_k)^t \mathbf{M}_k^{-1} (\beta^{\frac{1}{2}} \mathbf{A}_k + \mathbf{M}_k)$$

is used in place of \mathbf{S}_k , then the eigenvalues of $\widehat{\mathbf{S}}_k^{-1} \mathbf{S}_k$ are contained in the small interval $[\frac{1}{2}, 1]$, independently of the problem parameters. This estimate can be approximated in case the exact diagonal block $\widehat{\mathbf{S}}_k$ is in turn approximated as

$$\widetilde{\mathbf{S}}_k := \widetilde{\mathbf{P}}_k^t \mathbf{M}_k^{-1} \widetilde{\mathbf{P}}_k,$$

where $\widetilde{\mathbf{P}}_k$ is the multigrid operator for $\mathbf{P}_k = \beta^{\frac{1}{2}} \mathbf{A}_k + \mathbf{M}_k$. Indeed, the eigenvalues of $\widetilde{\mathbf{S}}_k^{-1} \mathbf{S}_k$ can be analyzed by writing the corresponding Rayleigh quotient as follows

$$\frac{\mathbf{v}^t \mathbf{S}_k \mathbf{v}}{\mathbf{v}^t \widetilde{\mathbf{S}}_k \mathbf{v}} = \frac{\mathbf{v}^t \mathbf{S}_k \mathbf{v}}{\mathbf{v}^t \widehat{\mathbf{S}}_k \mathbf{v}} \frac{\mathbf{v}^t \widehat{\mathbf{S}}_k \mathbf{v}}{\mathbf{v}^t \widetilde{\mathbf{S}}_k \mathbf{v}}.$$

The second factor yields

$$\frac{\mathbf{v}^t \widehat{\mathbf{S}}_k \mathbf{v}}{\mathbf{v}^t \widetilde{\mathbf{S}}_k \mathbf{v}} = \frac{\mathbf{v}^t \mathbf{P}_k^t \mathbf{M}_k^{-1} \mathbf{P}_k \mathbf{v}}{\mathbf{v}^t \widetilde{\mathbf{P}}_k^t \mathbf{M}_k^{-1} \widetilde{\mathbf{P}}_k \mathbf{v}} = \frac{\mathbf{u}^t (\mathbf{P}_k \widetilde{\mathbf{P}}_k^{-1})^t \mathbf{M}_k^{-1} \mathbf{P}_k \widetilde{\mathbf{P}}_k^{-1} \mathbf{u}}{\mathbf{u}^t \mathbf{M}_k^{-1} \mathbf{u}},$$

where $\mathbf{u} = \widetilde{\mathbf{P}}_k \mathbf{v}$, and

$$\sigma_{\min}(\mathbf{P}_k \widetilde{\mathbf{P}}_k^{-1})^2 \frac{1}{\text{cond}(\mathbf{M}_k)} \leq \frac{\mathbf{u}^t (\mathbf{P}_k \widetilde{\mathbf{P}}_k^{-1})^t \mathbf{M}_k^{-1} \mathbf{P}_k \widetilde{\mathbf{P}}_k^{-1} \mathbf{u}}{\mathbf{u}^t \mathbf{M}_k^{-1} \mathbf{u}} \leq \sigma_{\max}(\mathbf{P}_k \widetilde{\mathbf{P}}_k^{-1})^2 \text{cond}(\mathbf{M}_k).$$

Here $\sigma_{\min}(\cdot)$, $\sigma_{\max}(\cdot)$ are the minimum and maximum singular values of the argument matrix, and $\text{cond}(\cdot)$ is the spectral condition number of its argument. We recall that the condition number of \mathbf{M}_k remains very moderate, independently of the problem parameters. In summary, we have obtained the following estimates for the Rayleigh

quotient associated with $\mathbf{S}_k \tilde{\mathbf{S}}_k^{-1}$ and any nonzero vector \mathbf{v} ,

$$\frac{1}{2} \frac{\sigma_{\min}^2}{\text{cond}(\mathbf{M}_k)} \leq \frac{\mathbf{v}^t \mathbf{S}_k \mathbf{v}}{\mathbf{v}^t \tilde{\mathbf{S}}_k \mathbf{v}} \leq \sigma_{\max}^2 \cdot \text{cond}(\mathbf{M}_k);$$

(a short-hand notation is used for the singular values). The lower and upper bounds show that the quality of the multigrid operator in approximating the spectral properties of the convection-diffusion operator plays a crucial role for the spectral properties of the whole preconditioned system. Our extensive computational experimentation, some of which is reported below, seems to show that the designed multigrid operator achieves the goal of making these bounds parameter independent. A rigorous proof remains an important and challenging open problem.

5.1. Downwind ordering. It is well-known that reordering the unknowns is crucial for convection-dominated problems. For continuous Galerkin (CG) methods, we refer to [42, 5, 22] for more details. For DG methods, it was pointed out in [21] that downwind ordering of the elements makes the matrix representing the convection term block triangular. We briefly describe an algorithm to order the elements following the convection direction. First, we have the following definitions [27].

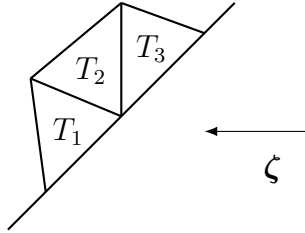


FIGURE 2. Boundary and semi-boundary elements

Definition 5.1 (Boundary elements). An element $T \in \mathcal{T}_h$ is a boundary element if and only if at least one of the edges of T belongs to $\partial\Omega$.

Definition 5.2 (Semi-boundary elements). An element $T \in \mathcal{T}_h$ is a semi-boundary element if and only if one of the vertices of T belongs to $\partial\Omega$.

Now we describe the downwind ordering algorithm as follows in Algorithm 1.

Example 5.3. In Figure 2, the elements T_1 and T_3 are boundary elements while T_2 is a semi-boundary element. Since the convection field ζ flows from right to left, the downwind ordering of the elements is T_3, T_2, T_1 .

Algorithm 1 Downwind ordering for DG methods

- 1: Find all the boundary elements on the inflow boundary $\mathcal{E}_h^{b,-}$ and all the semi-boundary elements that have vertices on the inflow boundary $\mathcal{E}_h^{b,-}$. Denote them as $\{T_i\}_{i=1}^N$.
 - 2: Reorder all the elements gathered in Step 1 such that the outflow boundary of T_i is the inflow boundary of T_j for $i < j$ if $T_i \cap T_j \neq \emptyset$.
 - 3: Exclude the elements $\{T_i\}_{i=1}^N$ from \mathcal{T}_h and repeat the process.
-

5.2. Multigrid methods for diffusion-convection-reaction equations. The design of multigrid methods for the diffusion-convection-reaction equations, especially in the convection-dominated regime, is not trivial. Usual components of multigrid would not work well for this problem. This was investigated extensively in [43, 34, 21, 25, 16]. One has to either use a specially designed smoothing step or reorder the unknowns following the flow direction. One key observation is that the smoother used in the multigrid should work for the case when $\varepsilon = 0$, i.e, the pure hyperbolic case [34]. Let us consider the state equation (1.2) and the corresponding discrete problem at the k th level,

$$(5.4) \quad \mathbf{A}_k \mathbf{w} = \mathbf{f},$$

where \mathbf{A}_k is the matrix represents $a_h(\cdot, \cdot)$ at the k th level. The following algorithm describes a V -cycle algorithm with the forward block Gauss-Seidel smoother \mathbf{G}_k using downwind ordering in Algorithm 1. Here \mathbf{I}_k^{k-1} and \mathbf{I}_{k-1}^k represent standard fine-to-coarse and coarse-to-fine operators respectively. Note that with downwind ordering, the matrix representing the convection term becomes block lower triangular, hence the forward block Gauss-Seidel smoother is efficient [27, 21]. In the case of linear polynomials, where the diagonal block is 3×3 , computing \mathbf{G}_k is highly efficient.

Algorithm 2 V -cycle algorithm for convection-dominated problem with downwind ordering with respect to $\boldsymbol{\zeta}$, $MG(k, \mathbf{f}, \mathbf{u}_0, m_1, m_2)$

- 1: Given initial guess \mathbf{u}_0 and \mathbf{f} .
 - 2: If $k = 0$, let $\mathbf{u} = \mathbf{A}_k^{-1} \mathbf{f}$, otherwise do the following,
 - 3: Pre-smoothing: For $i = 1$ to m_1 ,
 - 4: $\mathbf{u}_i = \mathbf{u}_{i-1} + \mathbf{G}_k(\mathbf{f} - \mathbf{A}_k \mathbf{u}_{i-1})$.
 - 5: Compute $\mathbf{r} = \mathbf{I}_k^{k-1}(\mathbf{f} - \mathbf{A}_k \mathbf{u}_{m_1})$.
 - 6: Set $\mathbf{r} = MG(k-1, \mathbf{f}, \mathbf{r}, m_1, m_2)$.
 - 7: Compute $\mathbf{u}_{m_1+1} = \mathbf{u}_{m_1} + \mathbf{I}_{k-1}^k \mathbf{r}$.
 - 8: Post-smoothing: For $i = m_1 + 2$ to $m_1 + m_2 + 1$,
 - 9: $\mathbf{u}_i = \mathbf{u}_{i-1} + \mathbf{G}_k(\mathbf{f} - \mathbf{A}_k \mathbf{u}_{i-1})$.
-

For the dual problem (1.6b), the downwind ordering with respect to $-\zeta$ makes the convection matrix block lower triangular. Hence, the forward block Gauss-Seidel smoother is also efficient for the dual problem.

Remark 5.4. We do not need to reorder the elements according to $-\zeta$ again. Once we have the downwind ordering $\{T_i\}_{i=1}^N$ with respect to ζ , the downwind ordering with respect to $-\zeta$ is $\{T_i\}_{i=N}^1$. We can then utilize this ordering to solve the dual problem efficiently.

5.3. Efficient implementation of the preconditioner (5.3). Combining the downwind ordering in Section 5.1 and the efficient multigrid methods in Section 5.2, we can compute the preconditioner (5.3) efficiently as follows in Algorithm 3.

Algorithm 3 Efficient computation of the preconditioner (5.3)

- 1: Given $\begin{pmatrix} \mathbf{w} \\ \mathbf{v} \end{pmatrix}$.
 - 2: Compute $\mathbf{w}_1 = \mathbf{M}_k^{-1}\mathbf{w}$. This step is exact since \mathbf{M}_k is block-diagonal.
 - 3: Compute $\mathbf{v}_1 = MG(k, \mathbf{v}, 0, m_1, m_2)$ (apply to $(\beta^{\frac{1}{2}}\mathbf{A}_k + \mathbf{M}_k)^t$).
 - 4: Compute $\mathbf{v}_2 = \mathbf{M}_k\mathbf{v}_1$.
 - 5: Compute $\mathbf{v}_3 = MG(k, \mathbf{v}_2, 0, m_1, m_2)$ (apply to $(\beta^{\frac{1}{2}}\mathbf{A}_k + \mathbf{M}_k)$).
 - 6: Output $\tilde{\mathcal{P}}_h^{-1} \begin{pmatrix} \mathbf{w} \\ \mathbf{v} \end{pmatrix} = \begin{pmatrix} \mathbf{w}_1 \\ \mathbf{v}_3 \end{pmatrix}$.
-

Remark 5.5. When ε is tiny, one forward block Gauss-Seidel sweep is enough for Step 3 and Step 5. Indeed, for the pure hyperbolic case, forward block Gauss-Seidel iteration is an exact solver [21]. Therefore, for strongly convection-dominated case, Algorithm 3 is extremely efficient.

6. NUMERICAL RESULTS

In this section, we show numerical experiments of the DG methods (3.16) and the corresponding preconditioner introduced in the previous section. We solve the discrete problem (3.16) using MINRES preconditioned by $\tilde{\mathcal{P}}_k$ defined in (5.3) with tolerance 10^{-6} . We use the built-in `minres` function in MATLAB to solve the discrete problem. Steps 3 and 5 in Algorithm 3 are computed by a single V-cycle multigrid method described in Algorithm 2 with 8 pre-smoothing and post-smoothing steps. To broaden our comparisons, we have also used an ILU-preconditioned BiCGSTAB(ℓ) algorithm (default code in Matlab) with tolerance 10^{-8} to compute Steps 3 and 5 in Algorithm 3 as well. In addition, for $\varepsilon = 10^{-6}$ and 10^{-9} , we also compute Step 3 and

TABLE 1. Example 6.1. Contraction numbers of multigrid methods for Step 5 in Algorithm 2 with $\beta = 1$ and different ε

k	$\varepsilon = 10^{-1}$			$\varepsilon = 10^{-3}$		
	m			m		
	2	4	8	2	4	8
1	9.27e-02	1.55e-02	4.53e-04	1.53e-07	3.12e-14	1.69e-16
2	1.73e-01	4.94e-02	5.84e-03	3.27e-05	6.45e-07	5.16e-16
3	2.55e-01	1.37e-01	4.61e-02	9.28e-04	1.67e-06	1.04e-12
4	3.19e-01	1.77e-01	9.04e-02	1.55e-02	1.72e-04	3.04e-08
5	3.63e-01	2.21e-01	1.19e-01	1.11e-01	8.44e-03	3.88e-05
6	3.81e-01	2.39e-01	1.32e-01	3.17e-01	1.00e-01	1.25e-02
7	3.98e-01	2.43e-01	1.41e-01	3.37e-01	1.72e-01	5.68e-02
k	$\varepsilon = 10^{-6}$			$\varepsilon = 10^{-9}$		
	m			m		
	2	4	8	2	4	8
1	2.44e-16	2.77e-16	2.83e-16	3.41e-16	2.98e-16	1.97e-16
2	4.85e-16	7.84e-16	4.82e-16	3.88e-16	3.60e-16	2.53e-16
3	6.68e-15	5.38e-16	5.66e-16	6.38e-16	5.34e-16	5.32e-16
4	1.68e-12	9.73e-16	1.05e-15	9.57e-16	1.24e-15	1.15e-15
5	3.80e-06	1.46e-15	1.73e-15	1.35e-15	1.63e-15	1.54e-15
6	3.18e-08	1.83e-15	1.86e-15	1.95e-15	2.16e-15	2.23e-15
7	2.74e-06	1.90e-11	2.69e-15	2.94e-15	2.89e-15	2.84e-15

Step 5 in Algorithm 3 with only one step of backward block Gauss-Seidel iteration and one step of forward block Gauss-Seidel iteration respectively.

We then include the convergence results in the convection-dominated regime to justify our main theorem. We denote $e_y = y - y_h$ and $e_p = p - p_h$ in this section, where y, p are solutions to (2.9) and p_h, y_h are solutions to the discrete problem (3.16). We compute the global convergence rates of the state and the adjoint state in L_2 and $\|\cdot\|_{1,\varepsilon}$ norms. We also compute the local convergence rates of the state and the adjoint state in L_2 and $\|\cdot\|_{H^1(\mathcal{T}_h)}$ norms. Here, the norm $\|\cdot\|_{H^1(\mathcal{T}_h)}$ is defined as $\|\cdot\|_{H^1(\mathcal{T}_h)}^2 := \sum_{T \in \mathcal{T}_h} \|\nabla \cdot\|_{H^1(T)}^2$. We then illustrate the efficiency of our preconditioner by showing the numbers of iteration for the preconditioned MINRES algorithm.

Example 6.1 (Multigrid Methods for Convection-dominated Problems). In this example, we first illustrate the contraction behaviors of the multigrid methods described in Algorithm 2. Note that Algorithm 2 is a crucial component of the preconditioner described in Algorithm 3. We compute the contraction numbers of the multigrid

methods for both the forward problem (Step 5 in Algorithm 3) and the dual problem (Step 3 in Algorithm 3) with m smoothing steps.

We first consider the case with different values of ε where $\beta = 1$. As one can see from Tables 1 and 2, our multigrid methods are highly efficient in convection-dominated regime, especially in the cases where $\varepsilon = 10^{-6}$ and $\varepsilon = 10^{-9}$. Indeed, as pointed out in [21], with downwind ordering, the block Gauss-Seidel iteration itself is almost a direct solver in these cases. For mild convection-dominated cases, where $\varepsilon = 10^{-3}$, one can see our multigrid methods also perform well. For the case $\varepsilon = 10^{-1}$, the convergence behavior of the multigrid methods tends to the classical $O(m^{-1})$ convergence rate as in the diffusion-dominated case. Overall, this example shows that, with downwind ordering, the multigrid methods with a block Gauss-Seidel smoother are extremely suitable for convection-dominated problems.

We then report the contraction numbers in Table 3 with different values of β where $\varepsilon = 10^{-3}$. For simplicity, we only include the results at higher levels for Step 5 in Algorithm 3. One can clearly see that the contraction numbers for Algorithm 2 are small for all β values, and they decrease when β decreases. This is because the block Gauss-Seidel algorithm tends to an exact solver with any ordering as $\beta \rightarrow 0$, due to the fact that \mathbf{M}_k is block-diagonal.

Example 6.2 (Smooth Solutions). In this example, we take $\Omega = [0, 1]^2$, $\gamma = 0$, $\zeta = [1, 0]^t$ and let the exact solutions of (2.9) be

$$(6.1) \quad y = x_1(1 - x_1)x_2(1 - x_2) \quad \text{and} \quad p = \sin(2\pi x_1) \sin(2\pi x_2).$$

We take $\beta = 1$ unless otherwise stated.

We first report the global convergence results of the methods (3.16) with $\varepsilon = 10^{-9}$ in Table 4. We observe $O(h^2)$ convergence for $\|e_y\|_{L_2(\Omega)}$ and $\|e_p\|_{L_2(\Omega)}$. They are better than the theoretical results in Theorem 4.1, which is due to the smoothness of the solutions. Similar convergence behaviors were also observed in [3]. We also observe almost $O(h^2)$ convergence for $\|e_y\|_{1,\varepsilon}$ and $O(h^{\frac{3}{2}})$ convergence for $\|e_p\|_{1,\varepsilon}$. Again, due to the smoothness of the solutions, we see higher convergence rates in $\|e_y\|_{1,\varepsilon}$. We also test and report the local convergence results with $\varepsilon = 10^{-9}$ in Table 5. Here we measure the L_2 and $\|\cdot\|_{H^1(\mathcal{T}_h)}$ errors in the domain $[0.25, 0.75]^2$. One can clearly see optimal convergence rates in L_2 and $\|\cdot\|_{H^1(\mathcal{T}_h)}$ norms for both variables. This is consistent with the results in [29].

We then show the MINRES numbers of iterations in Table 6 for various ε and different implementations of the preconditioner. We clearly see that the preconditioner (5.3) is robust with respect to ε . Moreover, the performance of the multigrid

TABLE 2. Example 6.1. Contraction numbers of multigrid methods for Step 3 in Algorithm 2 with $\beta = 1$ and different ε

k	$\varepsilon = 10^{-1}$			$\varepsilon = 10^{-3}$		
	m			m		
	2	4	8	2	4	8
1	9.27e-02	1.55e-02	4.53e-04	1.08e-07	3.49e-14	3.59e-16
2	1.75e-01	4.18e-02	7.65e-03	9.37e-06	5.39e-07	4.45e-16
3	2.48e-01	1.19e-01	4.51e-02	1.21e-03	1.05e-06	1.09e-11
4	3.25e-01	1.80e-01	8.02e-02	1.70e-02	1.85e-04	2.97e-08
5	3.68e-01	2.28e-01	1.16e-01	9.06e-02	6.12e-03	4.42e-05
6	3.82e-01	2.41e-01	1.38e-01	2.44e-01	6.08e-02	8.76e-03
7	3.99e-01	2.47e-01	1.40e-01	3.35e-01	1.82e-01	6.35e-02
k	$\varepsilon = 10^{-6}$			$\varepsilon = 10^{-9}$		
	m			m		
	2	4	8	2	4	8
1	2.06e-16	2.13e-16	2.42e-16	2.62e-16	2.45e-16	4.18e-16
2	5.21e-16	3.77e-16	2.70e-16	5.89e-16	4.39e-16	5.41e-16
3	9.52e-15	8.57e-16	6.50e-16	6.54e-16	8.76e-16	9.90e-16
4	1.93e-12	9.85e-16	1.20e-15	9.74e-16	1.05e-15	1.12e-15
5	4.18e-06	1.35e-15	1.31e-15	1.55e-15	1.41e-15	1.46e-15
6	2.90e-08	2.11e-15	1.85e-15	2.17e-15	2.05e-15	1.99e-15
7	2.72e-06	2.08e-11	2.57e-15	3.29e-15	2.83e-15	3.28e-15

TABLE 3. Example 6.1. Contraction numbers of multigrid methods for Step 5 in Algorithm 2 with $\varepsilon = 10^{-3}$ and different values of β

k	$\beta = 10^{-1}$			$\beta = 10^{-2}$		
	m			m		
	2	4	8	2	4	8
5	1.07e-01	7.61e-03	2.79e-05	6.44e-02	4.00e-03	2.01e-05
6	2.61e-01	1.10e-01	9.25e-03	1.80e-01	5.80e-02	7.75e-03
7	3.22e-01	1.72e-01	5.75e-02	2.81e-01	1.40e-01	3.57e-02
k	$\beta = 10^{-4}$			$\beta = 10^{-8}$		
	m			m		
	2	4	8	2	4	8
5	5.84e-04	2.73e-07	1.42e-14	4.50e-11	4.98e-16	4.50e-16
6	2.08e-02	4.02e-04	1.16e-07	4.91e-08	5.32e-16	4.59e-16
7	9.50e-02	1.50e-02	5.73e-04	3.98e-07	7.27e-13	4.56e-16

implementation of the preconditioner matches with the behavior of the contraction numbers in Example 6.1. Indeed, for $\varepsilon = 10^{-6}$ and $\varepsilon = 10^{-9}$, the multigrid method is almost an exact solver, hence the MINRES numbers of iterations are identical to those of BiCGSTAB. For $\varepsilon = 10^{-3}$ and $\varepsilon = 10^{-1}$, the MINRES numbers of iterations are still bounded with respect to k which is consistent with the results in Example 6.1. We also see that for $\varepsilon = 10^{-6}$ and $\varepsilon = 10^{-9}$, one sweep of backward and forward block Gauss-Seidel is enough (see Remark 5.5).

Lastly, we report the MINRES numbers of iterations in Table 7 for various β and different implementations of the preconditioner. We take $\varepsilon = 10^{-3}$ in Table 7. One can see that the preconditioner is robust with respect to β as well.

TABLE 4. Convergence rates for Example 6.2 with $\varepsilon = 10^{-9}$ (Global)

k	$\ e_y\ _{L_2(\Omega)}$	Order	$\ e_y\ _{1,\varepsilon}$	Order	$\ e_p\ _{L_2(\Omega)}$	Order	$\ e_p\ _{1,\varepsilon}$	Order
1	1.11e-02	-	1.51e-02	-	5.25e-03	-	5.36e-03	-
2	5.55e-02	-2.32	5.76e-02	-1.93	1.42e-01	-4.76	2.51e-01	-5.55
3	1.48e-02	1.90	1.52e-02	1.92	3.58e-02	1.99	9.97e-02	1.33
4	3.78e-03	1.97	3.87e-03	1.98	8.92e-03	2.00	3.63e-02	1.46
5	9.50e-04	1.99	9.81e-04	1.98	2.23e-03	2.00	1.29e-02	1.49
6	2.38e-04	2.00	2.52e-04	1.96	5.57e-04	2.00	4.56e-03	1.50
7	5.94e-05	2.00	6.60e-05	1.93	1.39e-04	2.00	1.61e-03	1.50
8	1.49e-05	2.00	1.80e-05	1.88	3.48e-05	2.00	5.68e-04	1.50

TABLE 5. Convergence rates for Example 6.2 with $\varepsilon = 10^{-9}$ (Local)

k	$\ e_y\ _{L_2(\Omega)}$	Order	$\ e_y\ _{H^1(\mathcal{T}_h)}$	Order	$\ e_p\ _{L_2(\Omega)}$	Order	$\ e_p\ _{H^1(\mathcal{T}_h)}$	Order
1	2.95e-03	-	1.48e-02	-	1.64e-03	-	8.88e-03	-
2	1.01e-02	-1.77	1.13e-01	-2.94	3.60e-02	-4.45	4.60e-01	-5.69
3	5.16e-03	0.96	4.71e-02	1.26	1.51e-02	1.25	3.76e-01	0.29
4	1.52e-03	1.77	1.80e-02	1.39	4.09e-03	1.89	2.05e-01	0.88
5	4.01e-04	1.92	7.44e-03	1.27	1.05e-03	1.96	1.06e-01	0.96
6	1.03e-04	1.96	3.31e-03	1.17	2.67e-04	1.98	5.35e-02	0.98
7	2.60e-05	1.98	1.55e-03	1.10	6.72e-05	1.99	2.69e-02	0.99
8	6.54e-06	1.99	7.47e-04	1.05	1.69e-05	1.99	1.35e-02	0.99

TABLE 6. MINRES numbers of iterations for Example 6.2

k	MG				BGS		BiCGSTAB			
	ε									
	10^{-1}	10^{-3}	10^{-6}	10^{-9}	10^{-6}	10^{-9}	10^{-1}	10^{-3}	10^{-6}	10^{-9}
1	12	15	14	14	14	14	12	15	14	14
2	14	15	14	14	14	14	14	15	14	14
3	16	17	14	14	14	14	14	17	14	14
4	18	17	13	13	13	13	14	17	13	13
5	19	17	13	11	13	11	14	17	13	11
6	20	17	13	11	15	11	14	17	13	11
7	22	19	15	11	20	11	15	17	15	11

 TABLE 7. MINRES numbers of iterations for Example 6.2 with different values of β and $\varepsilon = 10^{-3}$

k	MG				BiCGSTAB			
	β							
	10^{-1}	10^{-2}	10^{-4}	10^{-8}	10^{-1}	10^{-2}	10^{-4}	10^{-8}
1	17	19	8	3	17	19	8	3
2	17	22	12	4	17	22	12	4
3	18	20	14	4	18	20	14	4
4	17	20	17	4	17	20	17	4
5	17	19	18	4	17	19	18	4
6	16	19	19	4	16	19	19	4
7	17	21	19	5	16	20	19	5

Example 6.3 (Boundary Layer). In this example, we take $\Omega = [0, 1]^2$, $\beta = 1$, $\gamma = 0$, $\zeta = [\sqrt{2}/2, \sqrt{2}/2]^t$ and let the exact solutions of (2.9) be $y = \eta(x)\eta(y)$ and $p = \eta(1-x)\eta(1-y)$, where

$$(6.2) \quad \eta(z) = z^3 - \frac{e^{\frac{z-1}{\varepsilon}} - e^{-1/\varepsilon}}{1 - e^{-1/\varepsilon}}.$$

It is known [29] that the solution y has a boundary layer near $x = 1$ and $y = 1$ and solution p has a boundary layer near $x = 0$ and $y = 0$, when ε goes to 0.

We first show the global convergence results of the methods (3.16) with $\varepsilon = 10^{-9}$ for Example 6.3. We can see from Table 8 that the global convergence of the state and the adjoint state is $O(h^{\frac{1}{2}})$ in L_2 and $\|\cdot\|_{1,\varepsilon}$ norms. These deteriorated convergence rates are caused by the sharp boundary layers presented near the outflow boundary.

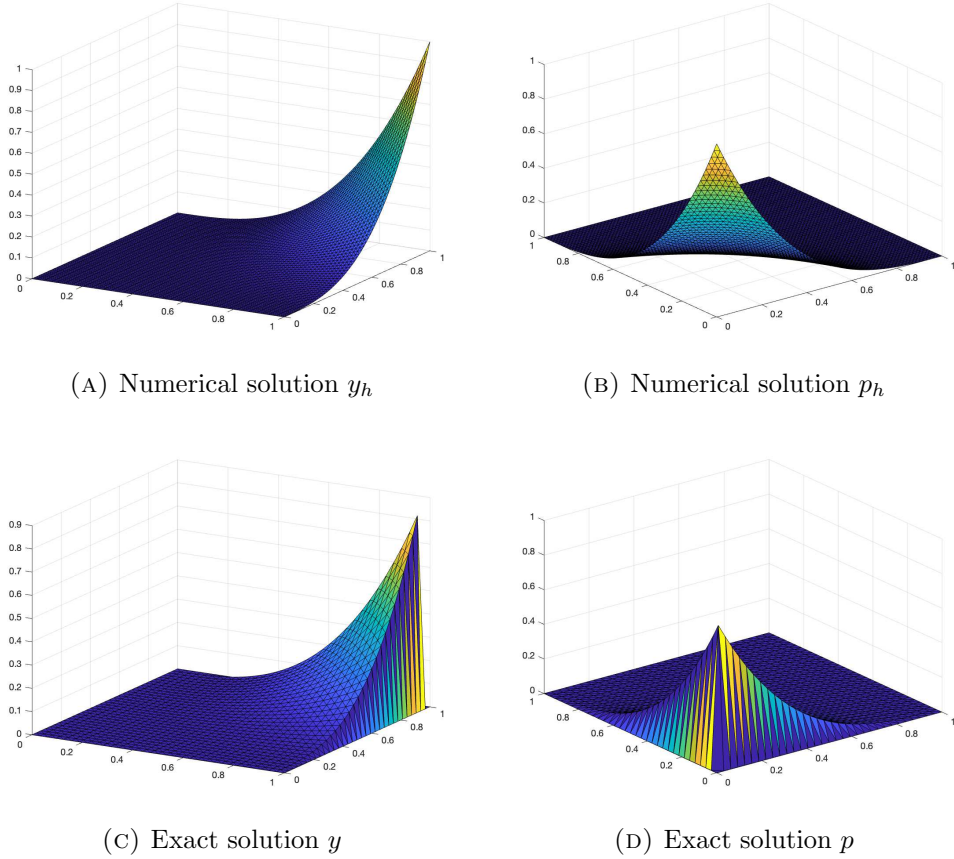


FIGURE 3. Numerical solutions and exact solutions

See Figure 3 for the comparison between numerical solutions and exact solutions. One can easily see that the boundary layers are ignored due to the weak treatment of the boundary conditions.

On the other hand, we measure the errors in the interior of the domain $[0.25, 0.75]^2$, which is away from the boundary layers. We found that the convergence rates are optimal in L_2 and $\|\cdot\|_{H^1(\mathcal{T}_h)}$ norms, as can be seen from Table 9. This illustrates the advantages of DG methods for optimal control problems, as the boundary layers do not pollute the solutions into the interior, where the solution is smooth (cf. [29]). Again, this is due to the fact that DG methods impose the boundary conditions weakly. This is in contrast to methods that impose the boundary conditions strongly, for example, the SUPG method [23], in which the oscillations propagate into the interior and one can at most expect $O(h)$ convergence for any polynomial degrees.

We then show the MINRES numbers of iterations in Table 10 for various ε and different implementations of the preconditioner. We again observe that the preconditioner (5.3) is robust with respect to ε . Similar MINRES numbers of iterations are observed for the multigrid preconditioner, as well as the block Gauss-Seidel iterations for small values of ε . We also report the MINRES numbers of iterations in Table 11 for different values of β . We again observe the robustness of the preconditioner with respect to β .

 TABLE 8. Convergence rates for Example 6.3 with $\varepsilon = 10^{-9}$ (Global)

k	$\ e_y\ _{L_2(\Omega)}$	Order	$\ e_y\ _{1,\varepsilon}$	Order	$\ e_p\ _{L_2(\Omega)}$	Order	$\ e_p\ _{1,\varepsilon}$	Order
1	1.33e-01	-	1.35e-01	-	1.35e-01	-	1.37e-01	-
2	1.28e-01	0.06	1.29e-01	0.07	1.29e-01	0.07	1.30e-01	0.08
3	1.03e-01	0.32	1.03e-01	0.32	1.03e-01	0.32	1.03e-01	0.33
4	7.59e-02	0.44	7.59e-02	0.44	7.59e-02	0.44	7.59e-02	0.44
5	5.43e-02	0.48	5.43e-02	0.48	5.43e-02	0.48	5.43e-02	0.48
6	3.85e-02	0.50	3.85e-02	0.50	3.85e-02	0.50	3.85e-02	0.50
7	2.73e-02	0.50	2.73e-02	0.50	2.73e-02	0.50	2.73e-02	0.50
8	1.93e-02	0.50	1.93e-02	0.50	1.93e-02	0.50	1.93e-02	0.50

 TABLE 9. Convergence rates for Example 6.3 with $\varepsilon = 10^{-9}$ (Local)

k	$\ e_y\ _{L_2(\Omega)}$	Order	$\ e_y\ _{H^1(\mathcal{T}_h)}$	Order	$\ e_p\ _{L_2(\Omega)}$	Order	$\ e_p\ _{H^1(\mathcal{T}_h)}$	Order
1	3.86e-03	-	2.16e-02	-	2.58e-03	-	1.57e-02	-
2	5.88e-04	2.72	7.19e-03	1.59	3.08e-04	3.07	4.25e-03	1.88
3	3.67e-04	0.68	6.06e-03	0.25	1.86e-04	0.72	6.10e-03	-0.52
4	1.32e-04	1.48	4.18e-03	0.54	6.97e-05	1.42	4.40e-03	0.47
5	3.88e-05	1.76	2.46e-03	0.77	2.09e-05	1.74	2.60e-03	0.76
6	1.05e-05	1.88	1.33e-03	0.88	5.72e-06	1.87	1.41e-03	0.89
7	2.74e-06	1.94	6.93e-04	0.94	1.49e-06	1.94	7.31e-04	0.94
8	6.98e-07	1.97	3.53e-04	0.97	3.81e-07	1.97	3.73e-04	0.97

Example 6.4 (Interior Layer). In this example, we take $\Omega = [0, 1]^2$, $\gamma = 0$, $\zeta = [1, 0]^t$ and let the exact solutions of (2.9) be

$$(6.3) \quad y = (1 - x_1)^3 \arctan\left(\frac{x_2 - 0.5}{\varepsilon}\right) \quad \text{and} \quad p = x_1(1 - x_1)x_2(1 - x_2).$$

TABLE 10. MINRES number of iterations for Example 6.3

k	MG				BGS		BiCGSTAB			
	ε									
	10^{-1}	10^{-3}	10^{-6}	10^{-9}	10^{-6}	10^{-9}	10^{-1}	10^{-3}	10^{-6}	10^{-9}
1	12	13	13	13	13	13	12	13	13	13
2	13	15	16	16	16	16	13	15	16	16
3	16	17	17	17	17	17	14	17	17	17
4	18	17	19	19	19	19	15	17	19	19
5	20	19	19	19	19	19	16	19	19	19
6	22	22	20	20	20	20	16	20	20	20
7	24	23	20	20	26	20	17	20	20	20

TABLE 11. MINRES numbers of iterations for Example 6.3 with different values of β and $\varepsilon = 10^{-3}$

k	MG				BiCGSTAB			
	β							
	10^{-1}	10^{-2}	10^{-4}	10^{-8}	10^{-1}	10^{-2}	10^{-4}	10^{-8}
1	15	18	11	5	15	18	11	5
2	18	22	14	5	18	22	14	5
3	20	23	17	5	20	23	17	5
4	21	23	21	5	21	23	21	5
5	21	25	23	6	21	25	23	6
6	24	25	24	8	22	25	24	8
7	27	27	24	11	22	25	24	11

The exact state y has an interior layer along the line $x_2 = 0.5$ for small ε . We take $\beta = 1$ unless otherwise stated.

We show the global convergence results for $\varepsilon = 10^{-9}$ in Table 12. We see that the convergence rates in L_2 norm for the state and the adjoint state are $O(h^{\frac{3}{2}})$, which coincide with Theorem 4.1. We also observe $O(h)$ convergence for the state in $\|\cdot\|_{1,\varepsilon}$ norm, which is caused by the interior layer. The convergence rate of the adjoint state in $\|\cdot\|_{1,\varepsilon}$ norm is $O(h^{\frac{3}{2}})$ which is optimal in the sense of Remark 4.2. The local convergence results in Table 13 are measured in the domain $[0.6, 1] \times [0, 1]$. The rates are all optimal in L_2 and $\|\cdot\|_{H^1(\mathcal{T}_h)}$ norms, which again, shows that the interior layer does not pollute the solutions into the domain where the solutions are smooth.

We then show the MINRES numbers of iterations in Tables 14 and 15 for various values of ε and β respectively as well as for different implementations of the preconditioner. Similar results are observed as those of previous examples.

TABLE 12. Convergence rates for Example 6.4 with $\varepsilon = 10^{-9}$ (Global)

k	$\ e_y\ _{L_2(\Omega)}$	Order	$\ e_y\ _{1,\varepsilon}$	Order	$\ e_p\ _{L_2(\Omega)}$	Order	$\ e_p\ _{1,\varepsilon}$	Order
1	1.92e-01	-	2.14e-01	-	9.13e-02	-	9.41e-02	-
2	6.80e-02	1.50	9.03e-02	1.24	3.18e-02	1.52	3.25e-02	1.54
3	2.27e-02	1.58	3.87e-02	1.22	1.09e-02	1.55	1.11e-02	1.55
4	7.67e-03	1.57	1.75e-02	1.14	3.74e-03	1.54	3.80e-03	1.54
5	2.63e-03	1.54	8.27e-03	1.08	1.30e-03	1.53	1.32e-03	1.53
6	9.16e-04	1.52	4.01e-03	1.04	4.54e-04	1.51	4.61e-04	1.51
7	3.21e-04	1.51	1.97e-03	1.02	1.60e-04	1.51	1.62e-04	1.51
8	1.13e-04	1.51	9.78e-04	1.01	5.64e-05	1.50	5.73e-05	1.50

TABLE 13. Convergence rates for Example 6.4 with $\varepsilon = 10^{-9}$ (Local)

k	$\ e_y\ _{L_2(\Omega)}$	Order	$\ e_y\ _{H^1(\mathcal{T}_h)}$	Order	$\ e_p\ _{L_2(\Omega)}$	Order	$\ e_p\ _{H^1(\mathcal{T}_h)}$	Order
1	1.46e-01	-	5.40e-01	-	7.54e-02	-	3.02e-01	-
2	4.62e-02	1.65	3.48e-01	0.64	2.14e-02	1.82	1.44e-01	1.07
3	5.85e-03	2.98	7.37e-02	2.24	2.42e-03	3.14	1.84e-02	2.97
4	1.53e-03	1.93	3.69e-02	1.00	6.41e-04	1.92	7.38e-03	1.32
5	3.91e-04	1.97	1.84e-02	1.00	1.65e-04	1.96	3.15e-03	1.23
6	9.67e-05	2.02	9.02e-03	1.03	4.08e-05	2.01	1.40e-03	1.17
7	2.40e-05	2.01	4.46e-03	1.02	1.02e-05	2.01	6.53e-04	1.10
8	6.02e-06	2.00	2.23e-03	1.00	2.55e-06	1.99	3.16e-04	1.05

7. CONCLUDING REMARKS

We have proposed and analyzed discontinuous Galerkin methods for an optimal control problem constrained by a convection-dominated problem. Optimal estimates are obtained and an effective multigrid preconditioner has been developed to solve the discretized system. Numerical results indicate that our preconditioner is robust with respect to β and ε . However, theoretical justification of the robustness of our methods seems nontrivial. This will be investigated in a future project.

TABLE 14. MINRES number of iterations for Example 6.4

k	MG				BGS		BiCGSTAB			
	ε									
	10^{-1}	10^{-3}	10^{-6}	10^{-9}	10^{-6}	10^{-9}	10^{-1}	10^{-3}	10^{-6}	10^{-9}
1	12	15	14	14	14	14	12	15	14	14
2	14	15	14	14	14	14	14	15	14	14
3	16	15	13	13	13	13	14	15	13	13
4	18	15	13	13	13	13	14	15	13	13
5	18	15	11	11	11	11	14	15	11	11
6	20	17	11	11	13	11	14	15	11	11
7	22	19	13	11	17	11	14	15	13	11

TABLE 15. MINRES numbers of iterations for Example 6.4 with different values of β and $\varepsilon = 10^{-3}$

k	MG				BiCGSTAB			
	β							
	10^{-1}	10^{-2}	10^{-4}	10^{-8}	10^{-1}	10^{-2}	10^{-4}	10^{-8}
1	18	20	9	3	18	20	9	3
2	19	22	12	4	19	22	12	4
3	19	22	17	4	19	22	17	4
4	21	23	21	4	21	23	21	4
5	20	25	23	6	20	25	23	6
6	21	25	25	7	20	25	25	7
7	22	26	26	10	20	25	26	10

Our approach can also be easily extended to higher order DG methods assuming higher regularity of the solutions. One only needs to replace the projection estimates (4.3) and (4.4) with

$$\|z - \pi_h z\|_{L_2(\Omega)} + h \|z - \pi_h z\|_d \lesssim h^{l+1} \|z\|_{H^{l+1}(\Omega)} \quad \forall z \in V,$$

$$\|z - \pi_h z\|_{ar} \lesssim (\tau_c^{-\frac{1}{2}} h^{l+1} + \|\zeta\|_{0,\infty}^{\frac{1}{2}} h^{l+\frac{1}{2}}) \|z\|_{H^{l+1}(\Omega)} \quad \forall z \in V,$$

and proceed with the same argument as that of Theorem 4.1. Here the integer $l > 1$ is the degree of the polynomials. We then obtain the following estimate which is similar to (4.5),

$$\begin{aligned} & \| \|p - p_h\| \| + \| \|y - y_h\| \| \\ & \lesssim C_{\dagger} \left(\beta^{\frac{1}{4}} (\varepsilon^{\frac{1}{2}} + \|\zeta\|_{0,\infty}^{\frac{1}{2}} h^{\frac{1}{2}} + \tau_c^{-\frac{1}{2}} h) h^l + h^{l+1} \right) (\|p\|_{H^{l+1}(\Omega)} + \|y\|_{H^{l+1}(\Omega)}). \end{aligned}$$

Our experiments have included BiCGSTAB(ℓ) as building block for our preconditioner for comparison purposes. Although the MINRES numbers of iterations by using BiCGSTAB(ℓ) were often the same as those of the multigrid operator, we emphasize that multigrid should still be preferred in practice. Indeed, BiCGSTAB is a nonlinear solver because it also depends on the right-hand side, so that the convergence of MINRES may be significantly affected by the BiCGSTAB solution accuracy. Moreover, BiCGSTAB depends on parameters such as a truncation and fill-in thresholds in its own ILU preconditioner. In contrast, multigrid may be used as a black box operator, and is an optimal $O(n)$ algorithm, where n is the number of unknowns. We expect multigrid to outperform BiCGSTAB(ℓ) when $h \rightarrow 0$ in terms of computational time.

ACKNOWLEDGEMENT

This material is based upon work supported by the National Science Foundation under Grant No. DMS-1929284 while the authors were in residence at the Institute for Computational and Experimental Research in Mathematics in Providence, RI, during the Numerical PDEs: Analysis, Algorithms, and Data Challenges semester program.

Part of the work of VS was funded by the European Union - NextGenerationEU under the National Recovery and Resilience Plan (PNRR) - Mission 4 Education and research - Component 2 From research to business - Investment 1.1 Notice Prin 2022 - DD N. 104 of 2/2/2022, entitled “Low-rank Structures and Numerical Methods in Matrix and Tensor Computations and their Application”, code 20227PCCKZ – CUP J53D23003620006. VS is member of the INdAM Research Group GNCS; its continuous support is gladly acknowledged.

REFERENCES

- [1] D. N. Arnold. An interior penalty finite element method with discontinuous elements. *SIAM Journal on Numerical Analysis*, 19(4):742–760, 1982.
- [2] D. N. Arnold, F. Brezzi, B. Cockburn, and L. Marini. Unified analysis of discontinuous Galerkin methods for elliptic problems. *SIAM Journal on Numerical Analysis*, 39(5):1749–1779, 2002.
- [3] B. Ayuso and L. D. Marini. Discontinuous Galerkin methods for advection-diffusion-reaction problems. *SIAM Journal on Numerical Analysis*, 47(2):1391–1420, 2009.
- [4] I. Babuška. The finite element method with Lagrangian multipliers. *Numerische Mathematik*, 20(3):179–192, 1973.
- [5] J. Bey and G. Wittum. Downwind numbering: Robust multigrid for convection-diffusion problems. *Applied Numerical Mathematics*, 23(1):177–192, 1997.
- [6] S. C. Brenner, H. Li, and L.-Y. Sung. Multigrid methods for saddle point problems: Stokes and Lamé systems. *Numerische Mathematik*, 128(2):193–216, 2014.
- [7] S. C. Brenner, H. Li, and L.-Y. Sung. Multigrid methods for saddle point problems: Oseen system. *Computers & Mathematics with Applications*, 74(9):2056–2067, 2017.

- [8] S. C. Brenner, S. Liu, and L.-Y. Sung. Multigrid methods for saddle point problems: Optimality systems. *Journal of Computational and Applied Mathematics*, 372, 2020.
- [9] S. C. Brenner, D.-S. Oh, and L.-Y. Sung. Multigrid methods for saddle point problems: Darcy systems. *Numerische Mathematik*, 138(2):437–471, 2018.
- [10] S. C. Brenner and L. R. Scott. *The Mathematical Theory of Finite Element Methods*, volume 15. Springer Science & Business Media, 2008.
- [11] F. Brezzi. On the existence, uniqueness and approximation of saddle-point problems arising from Lagrangian multipliers. *Revue française d'automatique, informatique, recherche opérationnelle. Analyse numérique*, 8(R2):129–151, 1974.
- [12] F. Brezzi, L. D. Marini, and E. Süli. Discontinuous Galerkin methods for first-order hyperbolic problems. *Mathematical models and methods in applied sciences*, 14(12):1893–1903, 2004.
- [13] P. Ciarlet. *The Finite Element Method for Elliptic Problems*, volume 19. 1978.
- [14] P. Ciarlet. Analysis of the Scott–Zhang interpolation in the fractional order sobolev spaces. *Journal of Numerical Mathematics*, 21(3):173–180, 2013.
- [15] D. A. Di Pietro and A. Ern. *Mathematical aspects of discontinuous Galerkin methods*, volume 69. Springer Science & Business Media, 2011.
- [16] H. C. Elman, D. J. Silvester, and A. J. Wathen. *Finite elements and fast iterative solvers: with applications in incompressible fluid dynamics*. Oxford university press, 2014.
- [17] A. Ern and J.-L. Guermond. Finite element quasi-interpolation and best approximation. *ESAIM: Mathematical Modelling and Numerical Analysis*, 51(4):1367–1385, 2017.
- [18] V. Faber, T. A. Manteuffel, and S. V. Parter. On the theory of equivalent operators and application to the numerical solution of ununiform elliptic partial differential equations. *Advances in Applied Mathematics*, 11:109–163, 1990.
- [19] F. Gaspoz, C. Kreuzer, A. Veaser, and W. Wollner. Quasi-best approximation in optimization with PDE constraints. *Inverse Problems*, 36(1):014004, 2019.
- [20] W. Gong, Z. Tan, and Z. Zhou. Optimal convergence of finite element approximation to an optimization problem with PDE constraint. *Inverse Problems*, 38(4):045004, 2022.
- [21] J. Gopalakrishnan and G. Kanschat. A multilevel discontinuous Galerkin method. *Numerische Mathematik*, 95(3):527–550, 2003.
- [22] W. Hackbusch and T. Probst. Downwind gauss-seidel smoothing for convection dominated problems. *Numerical linear algebra with applications*, 4(2):85–102, 1997.
- [23] M. Heinkenschloss and D. Leykekhman. Local error estimates for SUPG solutions of advection-dominated elliptic linear-quadratic optimal control problems. *SIAM Journal on Numerical Analysis*, 47(6):4607–4638, 2010.
- [24] M. Hinze. A variational discretization concept in control constrained optimization: the linear-quadratic case. *Computational Optimization and Applications*, 30:45–61, 2005.
- [25] H. Kim, J. Xu, and L. Zikatanov. Uniformly convergent multigrid methods for convection–diffusion problems without any constraint on coarse grids. *Advances in Computational Mathematics*, 20:385–399, 2004.
- [26] P. Knabner and L. Angermann. *Numerical methods for elliptic and parabolic partial differential equations: an applications-oriented introduction*. Springer, 2004.
- [27] P. Lesaint and P.-A. Raviart. On a finite element method for solving the neutron transport equation. *Publications des séminaires de mathématiques et informatique de Rennes*, (S4):1–40, 1974.

- [28] D. Leykekhman. Investigation of commutative properties of discontinuous Galerkin methods in PDE-constrained optimal control problems. *Journal of Scientific Computing*, 53(3):483–511, 2012.
- [29] D. Leykekhman and M. Heinkenschloss. Local error analysis of discontinuous Galerkin methods for advection-dominated elliptic linear-quadratic optimal control problems. *SIAM Journal on Numerical Analysis*, 50(4):2012–2038, 2012.
- [30] J. L. Lions. *Optimal Control of Systems Governed by Partial Differential Equations*. Springer, 1971.
- [31] S. Liu. Robust multigrid methods for discontinuous Galerkin discretizations of an elliptic optimal control problem. *Computational Methods in Applied Mathematics*, (0), 2024.
- [32] K.-A. Mardal, J. Sogn, and S. Takacs. Robust preconditioning and error estimates for optimal control of the convection–diffusion–reaction equation with limited observation in isogeometric analysis. *SIAM Journal on Numerical Analysis*, 60(1):195–221, 2022.
- [33] J. Nitsche. Über ein Variationsprinzip zur Lösung von Dirichlet-Problemen bei Verwendung von Teilräumen, die keinen Randbedingungen unterworfen sind. In *Abhandlungen aus dem mathematischen Seminar der Universität Hamburg*, volume 36, pages 9–15. Springer, 1971.
- [34] M. A. Olshanskii and A. Reusken. Convergence analysis of a multigrid method for a convection-dominated model problem. *SIAM Journal on Numerical Analysis*, 42(3):1261–1291, 2004.
- [35] J. Pearson and A. Wathen. Fast iterative solvers for convection-diffusion control problems. 2011.
- [36] B. Rivière. *Discontinuous Galerkin methods for solving elliptic and parabolic equations: theory and implementation*. SIAM, 2008.
- [37] J. Schöberl, R. Simon, and W. Zulehner. A robust multigrid method for elliptic optimal control problems. *SIAM Journal on Numerical Analysis*, 49(4):1482–1503, 2011.
- [38] J. Schöberl and W. Zulehner. Symmetric indefinite preconditioners for saddle point problems with applications to PDE-constrained optimization problems. *SIAM Journal on Matrix Analysis and Applications*, 29(3):752–773, 2007.
- [39] R. Simon and W. Zulehner. On Schwarz-type smoothers for saddle point problems with applications to PDE-constrained optimization problems. *Numerische Mathematik*, 111(3):445–468, 2009.
- [40] S. Takacs and W. Zulehner. Convergence analysis of multigrid methods with collective point smoothers for optimal control problems. *Computing and Visualization in Science*, 14(3):131–141, 2011.
- [41] F. Tröltzsch. *Optimal Control of Partial Differential Equations: Theory, Methods, and Applications*, volume 112. American Mathematical Soc., 2010.
- [42] F. Wang and J. Xu. A crosswind block iterative method for convection-dominated problems. *SIAM Journal on Scientific Computing*, 21(2):620–645, 1999.
- [43] C.-T. Wu and H. C. Elman. Analysis and comparison of geometric and algebraic multigrid for convection-diffusion equations. *SIAM Journal on Scientific Computing*, 28(6):2208–2228, 2006.
- [44] H. Yücel, M. Heinkenschloss, and B. Karasözen. Distributed optimal control of diffusion-convection-reaction equations using discontinuous Galerkin methods. In *Numerical Mathematics and Advanced Applications 2011: Proceedings of ENUMATH 2011, the 9th European Conference on Numerical Mathematics and Advanced Applications, Leicester, September 2011*, pages 389–397. Springer, 2012.

THE INSTITUTE FOR COMPUTATIONAL AND EXPERIMENTAL RESEARCH IN MATHEMATICS,
BROWN UNIVERSITY, PROVIDENCE, RI, USA

Email address: `sjing_liu@brown.edu`

DIPARTIMENTO DI MATEMATICA AND (AM)², ALMA MATER STUDIORUM - UNIVERSITÀ DI
BOLOGNA, 40126 BOLOGNA, AND IMATI-CNR, PAVIA, ITALY

Email address: `valeria.simoncini@unibo.it`